Published in final edited form as:
J Mol Biol. 2010 June 18; 399(4): 547–561. doi:10.1016/j.jmb.2010.04.036.

Interactions between late acting proteins required for peptidoglycan synthesis during sporulation

Allison Fay, **Pablo Meyer**, and **Jonathan Dworkin**
Department of Microbiology and Immunology, College of Physicians and Surgeons, Columbia University, New York, NY 10032

Abstract

The requirement of peptidoglycan synthesis for growth complicates the analysis of interactions between proteins involved in this pathway. In particular, the later steps that involve membrane-linked substrates have proven largely recalcitrant to *in vivo* analysis. Here we have taken advantage of the peptidoglycan synthesis that occurs during sporulation in *Bacillus subtilis* to examine the interactions between SpoVE, a non-essential, sporulation-specific homolog of the well-conserved and essential SEDS proteins, and SpoVD, a non-essential class B penicillin binding protein (PBP). We found that localization of SpoVD is dependent on SpoVE and that SpoVD protects SpoVE from *in vivo* proteolysis. Co-immunoprecipitations and Fluorescence Resonance Energy Transfer experiments indicated that SpoVE and SpoVD interact and co-affinity purification in *E. coli* demonstrated that this interaction is direct. Finally, we generated a functional protein consisting of a SpoVE-SpoVD fusion and found that a loss-of-function point mutation in either part of the fusion resulted in a loss of function of the entire fusion that was not complemented by a wild type protein. Thus, SpoVE has a direct and functional interaction with SpoVD and this conclusion will facilitate understanding the essential function SpoVE and related SEDS proteins such as FtsW and RodA play in bacterial growth and division.

Keywords

peptidoglycan; bacterial cell division; sporulation; bacterial growth

INTRODUCTION

Bacterial cell wall is composed of peptidoglycan, a rigid molecule that provides cells shape, protection, and scaffolding for extracellular proteins and structures. The peptidoglycan latticework is composed of glycan strands cross-linked by short peptides and is assembled on the outside of the cytoplasmic membrane. Synthesis of peptidoglycan begins in the cytoplasm where a series of conserved enzymes synthesize Lipid II, the membrane bound peptidoglycan precursor from a UDP-GlcNAc precursor.1 Lipid II, a disaccharide pentapeptide linked to an isoprenoid, must cross the membrane to undergo polymerization. Once it is flipped or translocated by an unknown mechanism, the disaccharides are polymerized and the peptides are cross-linked by penicillin binding proteins (PBPs).

Address correspondence to: Jonathan Dworkin, PhD, 701 W. 168th St., HHSC1218, New York, NY 10032, Fax: 212-305-1468, jonathan.dworkin@columbia.edu.

Members of the SEDS (Shape Elongation, Division, Septation) family are integral membrane proteins[2; 3; 4] that are typically essential and highly conserved among cell wall containing bacterial species.[5; 6] The SEDS proteins RodA and FtsW have been proposed to participate in the translocation of Lipid II during cell elongation and cell division, respectively.[7; 8] Depletion of *B. subtilis* RodA leads to a block in lateral cell growth.[6] A temperature sensitive *E. coli ftsW* mutation lead to blocks at both early and late stages of cell division,[9; 10] suggesting that FtsW acts during both initiation and septum maturation.[11] While absence of the sporulation-specific *B. subtilis* SEDS protein SpoVE leads to a block in spore peptidoglycan synthesis and an accumulation of soluble peptidoglycan precursors, [12] these experiments only indirectly demonstrate the precise function of SEDS proteins in peptidoglycan synthesis. However, a direct interaction between a SEDS protein and a protein such as a PBP that likely interacts with newly flipped substrate would be consistent with the proposed role of SEDS proteins in flipping.

Two distinct classes of PBPs have been characterized based on structure and function. Class A PBP proteins consist of a single N-terminal transmembrane helix and soluble domains for transglycosylation and transpeptidation.[13; 14; 15] While individual class A PBPs in *B. subtilis* and *E. coli* are not essential, this is likely due to functional redundancy with other Class A PBPs or with other soluble transglycosylases.[16; 17] In contrast, all known bacteria contain at least one essential class B PBP. These proteins are involved in cell septation, shape, and sporulation[18] and they consist of a single transmembrane helix, a transpeptidation domain and an additional soluble domain of unknown activity. While this transpeptidation activity has not been shown using natural substrates, it has been inferred from *in vitro* thioesterase activity[19; 20] and by *in vivo* analysis of cross-linking of mature peptidoglycan from mutant strains.[21] Thus, identification of the proteins that interact with class B PBPs would provide important clues as to why they are essential.

Peptidoglycan synthesis has been proposed to be mediated by separate elongation and division complexes that include one SEDS protein and PBPs.[8] The existence of multi-enzyme complexes containing PBPs has been reported in *H. influenzae*, although their precise molecular composition and organization is unknown.[22] Mutations in *E. coli ftsI* (encoding PBP3) that lead to a reduced ability to divide can be suppressed by *rodA* mutations that, by themselves, interfere with normal cell growth.[23] *E. coli* FtsW interacts with PBP3 in two different bacterial two hybrid assays.[24] In addition, FtsW from *Mycobacterium tuberculosis* interacts with PBP325 and proper localization of *E. coli* PBP3 to the septum is dependent on FtsW.[26]

Further analysis of these interactions has been complicated by the essential nature of most SEDS proteins and Class B PBPs. Interestingly, a non-essential process of peptidoglycan synthesis occurs during sporulation of *B. subtilis* where the spore cortex, a thick layer of peptidoglycan, is synthesized. This structure surrounds the spore and is necessary for spore heat resistance but not for spore formation itself. Mutations that prevent full-length protein expression in either *spoVE*, that encodes a non-essential SEDS protein,[27] or in *spoVD*, that encodes a non-essential class B PBP,[28] lead to the production of heat sensitive spores that lack a cortex.[29] SpoVE localizes to the forespore, the presumed site of peptidoglycan synthesis.[4] Sporulating *spoVE* and *spoVD* mutant strains accumulate soluble peptidoglycan precursors and exhibit a decrease in insoluble peptidoglycan produced, consistent with these *in vivo* observations.[12] Given that SpoVD and SpoVE are non-essential homologs of proteins that are in nearly all cases essential, cortex formation during sporulation offers a unique physiological context to assay their functional interaction.

RESULTS

SpoVD requires SpoVE for recruitment to the outer forespore membrane

The sporulation-specific penicillin-binding protein SpoVD functions in spore cortex peptidoglycan synthesis since *spoVD* mutations result in the production of heat sensitive spores lacking cortex28 and in the accumulation of peptidoglycan precursors.12 The *spoVD* gene is under the positive control of σ^E and the negative control of SpoIIID, two mother cell specific transcription factors.28; 30 Since SpoVE is recruited specifically to the outer forespore membrane 4 the likely site of spore cortex synthesis, we investigated the localization of SpoVD. We constructed an N-terminal GFP fusion and confirmed that it fully complemented the sporulation defect resulting from a *spoVD::kan* mutation (85 +/−7.2%). This strain was sporulated by resuspension and imaged at 3 hours (T3) post resuspension (Fig 1A, top). Since the fluorescence signal seen at the forespore membrane was most likely due to GFP-SpoVD localization at the outer forespore membrane, we calculated a ratio of average maximum forespore fluorescence to average maximum mother cell fluorescence as described for SpoVE.4 Consistent with our qualitative observations, GFP-SpoVD yielded a ratio of 3.27+/−.76, greater than the ratio expected (~2) if the protein is equally distributed in the mother cell membranes (Table 2).

We then asked about the requirement of other proteins for this localization pattern. While SEDS proteins are known to be required for the recruitment of *E. coli* class B PBPs31 and for *M. smegmatis* PBP3 which failed to be recruited to the division septa when FtsW was depleted,25 the essential nature of FtsW in these organisms complicates this analysis. We therefore investigated the requirement of SpoVE for proper SpoVD recruitment and observed that GFP-SpoVD was not preferentially recruited to the outer forespore membrane in a *ΔspoVE::tet* mutant background (Fig. 1A, bottom). The ratio of the average maximum forespore fluorescence to the average maximum mother cell fluorescence was 1.99 +/−.26 in a *ΔspoVE* background, a ratio that was significantly lower (p value <0.0001) than the ratio of 3.27 (+/−.76) observed in the wild type background (Table 2). Additionally, there were no obvious changes in the levels of GFP-SpoVD expression or in its proteolysis in a *ΔspoVE::tet* background as compared to the wild type background (Fig. 1B). Finally, a C-terminal fusion of mCherry to SpoVD (Fig. 1C) that was integrated at the endogenous locus exhibited a similar pattern of forespore localization as the N-terminal GFP-SpoVD fusion under control of P_{spoVe} (Fig 1A, top).

Several SpoVE point mutants localize and accumulate but result in a near-total reduction in spore heat resistance.4 To determine whether this defect resulted from the inability of these mutant proteins to appropriately recruit GFP-SpoVD, we placed each of the mutant *spoVE* alleles under their own promoter in a GFP-SpoVD expressing *ΔspoVE::tet* strain. However, all three SpoVE loss-of-function point mutants, G335A, G343A, and E271A, recruited GFP-SpoVD to the outer forespore membrane (Table 2), indicating that they were partially functional for some SpoVE functions although they were incapable of making spore cortex.

SpoVE requires SpoVD for stability in *B. subtilis* and in *E. coli*

Since appropriate localization of SpoVD was dependent on SpoVE, we examined whether the converse was also true. Introduction of a *spoVD::kan* null mutation into a strain that expresses a fully complementing SpoVE-GFP4 did not affect recruitment of SpoVE-GFP to the outer forespore membrane (data not shown). However, the absence of SpoVD did decrease the stability of SpoVE-GFP since anti-GFP immunoblotting revealed very little full-length protein (~55kDa), and instead a ~35kDa product that was presumably the result of proteolytic degradation of full-length SpoVE-GFP was observed (Fig. 2A). In lysates obtained from cultures grown until T3 of sporulation, this apparent cleavage product

comprised 85% (+/−7.8%) of the total signal for *spoVD::kan* background as compared to 20% (+/−3.0%) of the total signal for wild type. The stability defect of SpoVE-GFP was also observed during vegetative growth in wild type cells or in mutant cells lacking either FtsH, a membrane protease known to target integral membrane proteins,32 or seven other proteases (Apr, Vpr, Isp-1, Epr, Hpr, Bpr, Mpr)33 (data not shown). Thus, the absence of SpoVD results in SpoVE instability although the protease responsible for this degradation is not known.

Since very little full length SpoVE-GFP accumulates when it is expressed in *E. coli* BL21 under P_{ara} control (data not shown), we determined if SpoVD was sufficient to stabilize SpoVE in a heterologous expression system. While GST-SpoVD co-expression with SpoVE-GFP led to both an increase in accumulation of full-length protein and a decrease in cleavage product (Fig. 2B, left, lane 2), it did not stabilize *B. subtilis* FtsW (Fig. 2B, right, lane 2). This result suggests that a SEDS protein would be stabilized by the co-expression of a specific PBP partner. We therefore co-expressed the septation specific *B. subtilis* PBP2B34, the homolog of *E. coli* PBP3 that partners with FtsW,31 and found that it stabilizes *B. subtilis* FtsW as expected (Fig. 2B, right lane 3), it did not stabilize SpoVE (Fig. 2B, left lane 3). Thus, class B transpeptidases are capable of protecting specific SEDS proteins from proteolysis and suggests that the two proteins interact directly.

SpoVE and SpoVD co-immunoprecipitate from sporulating cells

The interaction between SpoVE and SpoVD in the recruitment and stability assays suggested that it was robust enough to be analyzed by co-immunoprecipitation. We therefore generated a strain expressing complementing SpoVD-FLAG and SpoVE-GFP fusions. This strain was sporulated by resuspension and lysates collected at T2.5 of sporulation were subjected to immunoprecipitation with M2 (anti-FLAG) affinity resin. Immunoblotting with anti-GFP revealed a doublet at approximately the position expected for SpoVE (~55 kDa), indicating that SpoVD was able to co-immunoprecipitate SpoVE (Fig. 3A, lane 3). The origins of this doublet are unclear, but the presence of 10 transmembrane domains in SpoVE could result in two species with slightly different electrophoretic mobilities. Heating lysates containing SpoVE-GFP to temperatures ranging from 37°C to 100°C resulted in decreasing mobility of SpoVE-GFP but increasing aggregation and loss of signal (data not shown). To examine whether this co-immunoprecipitation was specific to SpoVE, we generated a strain co-expressing SpoVD-FLAG and a complementing FtsW-GFP fusion. In contrast to SpoVE, SpoVD-FLAG did not co-immunoprecipitate FtsW-GFP (Fig. 3A, lane 4) despite the presence of both tagged proteins in the lysate (Fig. 3A, lane 4). This result was not unexpected since SpoVD was unable to protect FtsW from cleavage in *E. coli* (Fig. 3B). However, the failure of SpoVD and FtsW to co-immunoprecipitate indicates that an indirect or non-specific interaction did not occur. As an additional control for specificity, we generated a strain expressing both SpoVD-FLAG and a truncated form ($MalF_{(1,2)}$-GFP) of the heterologous membrane protein *E. coli* MalF.35 As with FtsW, this protein fusion was not co-immunoprecipitated by SpoVD-FLAG (Fig 3A, lane 2) despite the presence of $MalF_{(1,2)}$-GFP in the lysates (Fig 3A, lane 2). Finally, we generated a strain expressing a truncated version of the heterologous membrane protein *E. coli* $SecY_{(1,6)}$-FLAG and SpoVE-GFP, although no co-immunoprecipitation was observed despite the presence of $SecY_{(1,6)}$-FLAG in the lysates (Fig. 3A, lane 1). Taken together, these results demonstrate that the co-immunoprecipitation of SpoVE and SpoVD is specific.

SpoVE and SpoVD co-affinity purify in a heterologous system

The ability of SpoVD to stabilize SpoVE in *E. coli* (Fig. 3B) is consistent with a direct interaction. We used co-affinity purification in *E. coli* to examine this possibility and constructed an *E. coli* strain that co-expressed both an N-terminal fusion of SpoVD to

glutathione S-transferase (GST-SpoVD) and SpoVE-GFP under inducible control. A lysate from this strain was prepared and GST-SpoVD was affinity purified using immobilized glutathione resin. Immunoblotting with anti-GFP revealed the co-immunoprecipitation of SpoVE-GFP (Fig. 3B) indicating a direct interaction between the two proteins. This interaction was specific since SpoVE-GFP failed to co-purify with GST alone and GFP failed to co-purify with GST-SpoVD even though both proteins were present in the lysates (Fig. 3B). Thus, SpoVE and SpoVD form a stable complex in a heterologous system that is mediated by a direct protein-protein interaction.

Assay of the interaction between SpoVE and SpoVD in living *B. subtilis* cells

The pattern of enrichment of GFP-SpoVD at the outer forespore membrane is similar to that seen with SpoVE-GFP.4 To examine co-localization in the same cell, we constructed a *B. subtilis* strain expressing spectrally distinguishable YFP-SpoVD and SpoVE-CFP fusions. The fluorescent signals co-localized at the forespore at several time points in sporulation (Fig. 4A). However, such co-localizations are limited in resolution to λ/2 (for the peak of GFP emission at 508 nm, this is ~250 nm), and thus do not provide sufficient precision to determine that the two proteins are in close proximity. To obtain this information, we measured the FRET signal between the CFP and YFP fluorophores fused to each of the proteins. While the FRET signal is subject to a number of constraints including the orientation of the fluorophores, as well as the relative amounts of donor and acceptor proteins and the fraction of each protein that is in the complex, detections of much smaller distance (~10nm) is possible. When FRET occurs, the donor emits less photons as it de-excites by transferring the energy directly to the acceptor, so if the acceptor is photo-bleached, then donor fluorescence intensity increases.36 However, the magnitude of the FRET signal is simply reporting the efficiency of energy transfer and the physical proximity of the fluorophores is just one variable that determines this value.

Given these caveats, assay of intra-molecular FRET between fluorophores located on the same protein would suggest the (near-optimal) signal that could be expected from inter-molecular FRET. For the YFP-CFP tandem fusion protein under control of P_{spoVE}, we measured a FRET signal of −4.6 ± 4.5% (Fig. 4B). We then analyzed FRET between SpoVE-CFP and YFP-SpoVD fusions. The CFP and YFP molecules are likely located on the same face of the membrane since the N- and C-termini of SpoVE are cytoplasmic4 and a close homolog of SpoVD, *E. coli* PBP3, has a cytoplasmic N-terminus.37 We imaged cells at T2.5 of sporulation that were expressing SpoVE-CFP and YFP-SpoVD and measured the CFP intensities between consecutive sets of images taken at one-minute intervals, with and without photobleaching YFP. We then calculated the percentage difference in CFP intensity under the two conditions; if this quantity is negative, FRET is present. For SpoVE-CFP and YFP-SpoVD the difference was negative (mean = −5.8 ± 6.9%; Fig. 5B) indicating that CFP intensity was greater following YFP photobleaching and therefore FRET was occurring. Since this difference was similar to that measured with a YFP-CFP tandem fusion, SpoVE-CFP and YFP-SpoVD were likely in close proximity.

We demonstrated that this result was specific to the SpoVE-CFP/YFP-SpoVD pair by measuring the difference in several control strains. First, in a strain expressing SpoVE-CFP and free YFP, the difference in CFP intensity was positive (mean = 54.4 ± 16.0%; Fig. 4B) demonstrating that YFP must be fused to a membrane protein for FRET to be observed. We also measured a positive difference in CFP intensity (mean = 22.8 ± 7.6%; Fig. 4B) in a strain expressing SpoVE-CFP and FtsW-YFP indicating that FRET can not be detected between fluorophores fused to any two membrane proteins that are found in the same membrane.4 Thus, the FRET signal between SpoVE-CFP and YFP-SpoVD is consistent with the co-localization (Fig. 4A) and demonstrates that they are in proximity at T2.5 of sporulation.

We characterized the SpoVE and SpoVD interaction throughout sporulation by measuring FRET in samples taken every half-hour of a sporulating culture (Fig. 4C). We started at T2 when SpoVE-CFP and YFP-SpoVD fluorescence was first detectable (Fig. 4D). The difference in CFP fluorescence was negative at each time point from T2.5 to T4.5 indicating that two proteins were near each other during this interval (Fig. 4C). At T5 and T6, this difference was absent, indicating that they were likely no longer interacting. At T2, the population was mixed between FRET-positive and FRET-negative cells, perhaps because of the temporal heterogeneity of the sporulating cells. No negative values for the changes in CFP fluorescence were observed in a strain expressing free CFP and free YFP (Fig 4C).

A SpoVE-SpoVD protein fusion is functional

Both *Rhodococcus sp. RHA1*38 and *Solibacter usitatus* encode a protein that consists of a fusion of a SEDS protein and a class B PBP. For example, *Rhodococcus* RHA1_ro00248 (947 aa) has an N-terminal region with significant homology (e value = 4×10^{-29}) to the entire *B. subtilis* SpoVE (366 aa) SEDS and a C-terminal region with significant homology (e value = 1×10^{-40}) to nearly the entire *B. subtilis* class B PBP SpoVD (645 aa). We explicitly tested the possibility that a SEDS protein and a class B PBP can function as a single polypeptide chain by constructing a translational fusion of *spoVD* and *spoVE* with a sequence encoding a short linker composed of the amino acids GSGSGS inserted between the two ORFs and a C-terminal FLAG tag. This fusion was integrated into an ectopic site in the *B. subtilis* chromosome under control of P_{spoVE} and appeared at its expected size during sporulation (Supp. Fig. 2.). We assessed its functionality by measuring the heat resistance of spores since both *spoVD* and *spoVE* are necessary for spore heat resistance. Strains expressing the fusion protein and either the Δ*spoVE* or the *spoVD* mutations were sporulation proficient as was a strain expressing the fusion protein and carrying both mutations (Table 3). Thus, the SpoVE-SpoVD fusion protein was active both as a SEDS protein and as a PBP.

We determined whether this functionality was limited to fusions of sporulation-specific proteins by fusing the *B. subtilis* FtsW and PBP2B proteins that are each necessary for septum formation during vegetative growth.6; 34 The FtsW-PBP2B fusion was constructed similarly to the SpoVD-SpoVE fusion and was expressed at the predicted full-length size in growing cells under control of P_{ftsw} (data not shown). The fusion complemented both FtsW and PBP2B function since we could introduce both *ftsW::tet* and Δ*pbpB::mls* mutations into the strain expressing FtsW-PBP2B (JDB2440). We then asked whether a complementing fusion protein could be constructed where SpoVE is fused to PBP2B, a PBP with which it does not normally interact (Fig. 2B). That is, could the specificity we observed in the SEDS-PBP interaction be bypassed by a fusion that artificially tethered the two proteins? We observed, however, that a SpoVE-PBP2B fusion did not complement a Δ*spoVD* mutation (Table 3) despite being expressed appropriately during sporulation (data not shown). Thus, specificity cannot be bypassed simply by getting the PBP to the right place, but rather is the result of an interaction between a SEDS protein and its cognate PBP. Since this fusion did not complement the lack of heat resistance of Δ*spoVE* mutation (Table 3), tethering SpoVE to PBP2B prevented the SpoVE module from appropriately interacting with SpoVD.

We investigated whether the SpoVE-SpoVD fusion acted as a single functional unit or was capable of acting as a separate SEDS and PBP. That is, could we observe complementation *in trans* between a fusion protein carrying a loss-of-function mutation in one domain and either a single wild type SEDS or PBP? We used SpoVE loss-of-function point mutants that localized and accumulated4 and recruited SpoVD to the forespore (Table 2), indicating that they were somewhat competent for interaction with SpoVD. Introduction of these mutations (G335A, G343A, E271A) into the SpoVE-SpoVD fusion protein disabled its function because it failed to complement a Δ*spoVD* Δ*spoVE* mutation (Table 3). In addition, the

presence of a wild type copy of SpoVE did not allow the mutant fusion protein to complement a Δ*spoVD* mutation (Table 3). We confirmed that this failure of complementation was not due to expression defects since lysates revealed no significant differences in accumulation of the mutant fusion proteins (Fig. 5B). We then asked if these mutant fusion proteins were capable of localizing. A failure to localize to the outer forespore membrane could explain why the fusion failed to function. By using a SpoVE-SpoVD-mCherry fusion, we saw that wild type and fusions containing SpoVE(G335A) and SpoVE(G343A) still localized to the outer forespore membrane (Fig. 5A). Thus, the mutant SpoVE domain of the fusion was able to prevent the wild type SpoVD domain from properly functioning.

We used previously published alignments and mutational analysis of Class B PBPs39; 40 to identify residues of SpoVD likely to be essential for function. Importantly for this mutagenesis, SpoVD is a *non-essential* class B PBP homolog with a distinctive sporulation phenotype. Residue K496 of SpoVD is predicted to be located within active site box based on homology to PBP2B 41 and consistent with this prediction, GFP-SpoVD(K496A) failed to complement a *spoVD::kan* mutant as assayed by the lack of heat resistant spores (~0% heat resistant spores). We generated SpoVE-SpoVD fusion proteins carrying the severe loss-of-function SpoVD point mutation. Introduction of this mutation completely prevented complementation of the double Δ*spoVE spoVD* mutation (Table 3). Further, the presence of a wild type copy of SpoVD did not allow the mutant fusion proteins to complement a Δ*spoVE* mutation, indicating that the disabled SpoVD domain prevented the wild type SpoVE domain from functioning (Table 3). Localization of SpoVE-SpoVD(K496A)-mCherry showed that it was able to localize to the outer forespore membrane (Fig. 5A), and therefore a localization defect was unlikely to explain this failure to function.

In contrast to this result, introduction of the moderate SpoVD(Q227E) (~5% of wild type heat resistance; data not shown) mutation into the SpoVE-SpoVD fusion protein resulted in full complementation of the Δ*spoVE spoVD* double mutation (Table 3). Thus, tethering the partially inactive SpoVD(Q227E) protein to SpoVE restored its activity to wild type levels. This point mutation may prevent appropriate contacts between SpoVD and SpoVE and, consistent with this possibility, this residue is located on a surface exposed a-helix in a SpoVD homolog.42 Thus, the ability of the SpoVE-SpoVD fusion protein to complement a Δ*spoVE spoVD* double mutation and the inability of mutant alleles of this fusion to be complemented by the endogenous proteins strongly indicates that SpoVD and SpoVE interact directly.

DISCUSSION

Interaction of SpoVD and SpoVE

Like its homologs *S. pneumoniae* RodA and FtsW43 and *M. tuberculosis* FtsW,25 SpoVE is unstable. We found that SpoVD protected SpoVE from degradation in *B. subtilis* (Fig.2A) and in *E. coli* (Fig. 2B), suggesting that SpoVD-SpoVE interaction is direct. Although the septation-specific PBP2B was able to stabilize FtsW, it did not protect SpoVE, indicating that this interaction was highly specific (Fig 2B). When SpoVD-FLAG was used as bait in co-immunoprecipitation of lysates of sporulating *B. subtilis*, SpoVD pulled out SpoVE but not FtsW-GFP (Fig. 3A). We confirmed that this interaction was direct by demonstrating that tagged SpoVD immunoprecipitated SpoVE-GFP when both are expressed in *E. coli* (Fig. 3B). Taken together, these experiments demonstrate that SpoVD and SpoVE interact in a specific manner and that this interaction is direct. The strong sequence homology of SpoVD and SpoVE with their essential vegetative counterparts in both *B. subtilis* and in other bacteria, suggests this interaction is conserved with SEDS/PBP pairs such as FtsW/PBP2B.

Other membrane or membrane-associated proteins involved in peptidoglycan synthesis may be part of a larger complex that includes SpoVD and SpoVE. For example, minimal transglycosylation appears to be required for transpeptidation *in vitro*.44 A number of proteins with transglycosylase activity including class A PBPs and monofunctional enzymes have been characterized and, in fact, the *E. coli* class A PBP1B and class B PBP3 form a complex.45 In addition, the integral membrane protein MraY and the peripheral membrane proteins MurG proteins are responsible for the synthesis of Lipid I and Lipid II, respectively.1 Thus, such proteins would be components of a peptidoglycan synthetic complex and future experimental efforts will be directed at examining this possibility.

In vivo interaction of SpoVD and SpoVE

Although SpoVD and SpoVE appear to interact directly, the physiological role of this interaction is unclear. Since *spoVD* and *spoVE* mutations block spore cortex formation as seen by electron micrographs27;28 and by biochemical measurements of peptidoglycan synthesis,12 can their interaction in single cells be directly correlated with cortex formation? The observed co-localization of SpoVE-CFP and YFP-SpoVD suggests that this interaction occurs in sporulating cells (Fig. 4A). We confirmed this result with FRET, a higher resolution technique, and observed a FRET signal in individual cells expressing SpoVE-CFP and YFP-SpoVD (Fig. 4C) at times between T2.5 to T4.5 of sporulation during the period of spore cortex synthesis.46 A conclusive demonstration that this FRET signal is correlated with the putative function of these proteins would require the use of fluorescent probes to simultaneously visualize sites of active peptidoglycan synthesis.47; 48 However, these probes are not membrane permeable, and thus would not be able to access the site of spore cortex peptidoglycan synthesis in the membrane-bound compartment of the forespore.

Function of a single protein with both activities

The direct and stable interaction between SpoVD and SpoVE suggests that a single polypeptide consisting of a fusion of the two proteins would be functional. A synthetic fusion protein composed of the *E. coli* β and β′ subunits of RNA polymerase49 functions *in vivo*, consistent with the presence of an endogenous β-β′ fusion protein in *Helicobacter pylori*.50 Similarly, several bacterial ORFs encode a single large protein containing domains with significant homology to both SEDS and PBP proteins. We therefore constructed a SpoVE-SpoVD fusion and found that it complemented the double Δ*spoVD* Δ*spoVE* mutation (Table 3), indicating that the fusion exhibited the activities of each protein. A fusion constructed with the essential homologs FtsW-PBP2B similarly complemented null mutations in the genes encoding both the respective SEDS and PBP proteins. A fusion constructed using a non-cognate PBP (e.g., SpoVE-PBP2B) failed to complement the double mutation, indicating that simple tethering of a SEDS protein and a PBP was not sufficient.

The inability of SpoVE-SpoVD fusions carrying inactivating point mutations in either the SpoVE or the SpoVD domain to be complemented *in trans* by wild type proteins (Table 3) suggests a intimate interaction, perhaps as part of a macromolecular complex. If, as proposed previously for other SEDS proteins,8 SpoVE is a Lipid II flippase, then SpoVE would deliver intracellularly synthesized Lipid II to the extracellular SpoVD. However, given that transglycosylation and the concomitant removal of the lipid tail51 is thought to precede transpeptidation,52 this mechanism seems implausible. Therefore, the SpoVE/SpoVD complex could function so that SpoVD “catches” the newly flipped Lipid II on the extracellular face of the membrane and then “releases” these molecules to a class A PBP which would then covalently attach the flipped Lipid II molecules to mature peptidoglycan by transpeptidation and transglycosylation reactions. While this model is consistent with the lack of evidence for the transpeptidation of natural substrates by Class B PBPs, a current goal of our laboratory is the direct biochemical evaluation of mechanism.

MATERIALS AND METHODS

Bacterial and DNA manipulation

Plasmids (Supplemental Table S1) were constructed using standard methods. *B. subtilis* strains (Table 1) were derivatives of PY79 unless noted.53 *B. subtilis* was transformed using the two-step method 54 and sporulation was by resuspension.55 Spore heat resistance was assayed following sporulation by exhaustion in Difco nutrient broth medium (DSM) in 2ml cultures for 24 hours. Serial dilutions were plated before and after the cells were heated to 80°C for 20 min and CFUs compared to obtain % sporulation.

Co-immunoprecipitation

At T2.5 of sporulation by resuspension, each 25ml culture was collected by centrifugation and resuspended in 1ml SMM with 1mg/ml lysozyme. After incubating for 5 min at RT, the protoplasts were collected and lysed in 1ml solubilization buffer (50mM Tris, pH 7.5, 150mM NaCl, 1% NP-40, plus 200μM PMSF, 1μg/ml pepstatin A, 1μg/ml DNase I, 1μg/ml RNase A) and solubilized at 4°C for 1h. Insoluble material was removed by centrifugation (20,000 × g) for 30 min at 4°C and the supernatant (lysate) was added to 10μl of packed M2 affinity resin (Sigma) pre-washed with 50mM Tris, pH 7.5, 150mM NaCl, 0.5% NP-40 and allowed to bind for 1 hour at 4°C. The resin was then washed 5x with 1.5ml of buffer (50mM Tris, pH 7.5, 150mM NaCl, 0.5% NP-40) and samples were eluted with 50μl of 1x sample buffer at RT. The resin was pelleted and 15ml of the supernatant was subjected to 13.5% SDS-PAGE. Gels were transferred to Biotrace-NT (Pall) and probed using anti-GFP rabbit serum (gift of H. Shuman, 1:25000), anti-rabbit-HRP (1:25000, Pierce), then ECL plus (GE). Blots were then stripped and probed with anti-FLAG (polyclonal, 1:3000, Sigma), anti-rabbit-HRP (1:25000), then ECL plus.

Co-affinity purification

E. coli BL21 strains were grown in 100ml Luria broth (LB) with ampicillin (200μg/ml) and chloramphenicol (30μg/ml) at 37°C to an OD_{600}=0.8. Cultures were then cooled to RT and induced with 0.1% L-arabinose for 3h. Pellets were collected by centrifugation and frozen at −80°C. Pellets were thawed and resuspended in 5ml PBS (pH 7.5) with 0.2 mg/ml lysozyme, 200 mM PMSF, 1mg/ml pepstatin A, 1mg/ml DNase I, 1mg/ml RNase A, and incubated for 30 min at 4°C. Suspensions were briefly sonicated and all unbroken cells were pelleted by centrifugation (5,000 × g, 10 min). 1% NP-40 was added to the supernatant for 1h to solubilize the membranes. Insoluble material was collected by centrifugation (20,000 × g, 30 min) and the supernatant added to 25ml packed immobilized glutathione (Thermo) pre-washed with PBS and allowed to bind for 1 h. Resin was then washed 5x (10ml PBS, 0.5% NP-40) and eluted with 200ml 1x sample buffer at RT. The resin was pelleted and 15μl of supernatant was subjected to 13.5% SDS-PAGE. Gels were transferred to Biotrace-NT and probed using anti-GFP (1:3000, Zymed), anti-mouse-HRP (1:3000), then ECL plus. Blots were stripped and probed with anti-GST (1:3000, Sigma), anti-rabbit-HRP (1:25000), then ECL plus.

Immunoblot analysis of cell lysates

For *B. subtilis*, OD_{600} was taken at each time point, represented as hours post resuspension or post induction in LB. Volumes of samples were normalized to yield an OD_{600}=0.5. After pelleting, cells were resuspended and protoplasted in 100μl SMM with 1mg/ml lysozyme for 5 min at RT. Protoplasts were lysed after collection by resuspension in 100μl of 1x sample buffer and solubilized for 30 min at RT. 20μl of each sample was subjected to electrophoresis on a 13.5% or a 12% SDS-PAGE. Gels were transferred to Biotrace-NT and probed using anti-GFP rabbit serum (1:25000), anti-FLAG (polyclonal), or anti-RFP

(1:3000, Rockland Immunochemicals), then anti-rabbit-HRP (1:25000), then detected using ECL plus. As a control for σ^E activation during sporulation by resuspension, blots were stripped and probed with anti-YaaH, a protein whose expression is under control of σ^E 56. ImageJ (NIH) was used after scanning film. For *E. coli*, the OD_{600} following induction with 0.1% L-arabinose for 1h at RT was taken and volumes of samples were normalized to an OD_{600}=0.5. After pelleting, cells were resuspended and lysed in 1x sample buffer at RT. 15μl of each sample was electrophoresed on a 13.5% SDS-PAGE gel. Gels were transferred to Biotrace-NT and probed using anti-GFP (1:3000), anti-mouse-HRP (1:3000), and detected using ECL plus. Blots were then stripped and probed with anti-GST (1:3000), anti-rabbit-HRP (1:25000), and detected using ECL plus.

Fluorescence microscopy and localization quantification

100μl of sporulating cells were taken at designated times after resuspension. To each sample, 1μl of FM4-64 (100 μg/ml; Invitrogen) was added just before the cells were collected by centrifugation. For samples expressing mCherry fusions, FM4-64 was not added. The pellet was resuspended in 10μl PBS, and added to a poly-L-lysine pretreated coverslip. All microscopy was performed on a Nikon Eclipse 90i with a 100X phase contrast objective and captured by a Hamamatsu Orca-ER camera using Nikon Elements BR software. Exposures for FITC (GFP) images were 400ms and for TRITC (RFP and FM4-64) images were 800ms. Protein recruitment of SpoVE-GFP and GFP-SpoVD to the outer forespore membrane was quantified as described4 at T2.5 or T3 following resuspension. For each cell we measured the maximum GFP fluorescence along five lines across the middle of forespore and the maximum GFP fluorescence along five lines across the middle of the mother cell. We took the average maximum GFP fluorescence of the five lines for the forespore and mother cell for each cell and used these numbers to calculate the ratio of forespore to mother cell fluorescence. We repeated this for >200 cells from three experiments each strain tested. Sporulating cells selected at random represented both engulfing and engulfed forespores.

Generation of SpoVD point mutations

Mutations were introduced by two-step, PCR SOEing,57 in which complimentary oligonucleotides were designed containing the appropriate codon substitution and 15bp 3′ and 5′ to the codon changed. To generate the K496A mutation AFO553 and AFO553-r were used. To generate the Q227E mutation AFO593 and AFO593-r were used. Each oligonucleotide was used in a first round PCR with either ojd006 or AFO536 and pKM61 as template, containing P_{spoVE}-*gfp-spoVD*, to generate two products with overlapping regions. Each product was gel purified and then mixed at equal molar quantities and used as a template for a second round of PCR with ojd006 and AFO536. The final full-length product with the mutation of interest was digested with *EcoR*I and *BamH*I and ligated to pDG1662 digested with the same enzymes. Table S2 contains oligonucleotide sequences.

FRET by acceptor photobleaching

YFP images were taken using a cube (Chroma) containing 500/20nm (excitation), 515nm long pass dichroic, and 535/15nm (emission) filters. CFP images were taken using a cube (Chroma) containing 435/20 (excitation), 455nm long pass dichroic, and 480/40 (emission) filters. 3 sets of CFP/YFP images (500 ms each; T1, T2, T3) were taken at one min intervals. During the T1-T2 interval, the YFP was photo-bleached for one minute and bleaching was confirmed by comparing the T2 and T3 with the T1 YFP images. Percentile changes of CFP fluorescence for single cells between images T1 and T2 and images T2 and T3 were determined. A region of interest in each cell was selected and the mean background noise was subtracted for both CFP and YFP channels. The FRET signal was calculated as follows: $(CFP_{T1}\text{-}CFP_{T2})/CFP_{T1}$ - $(CFP_{T2}\text{-}CFP_{T3})/CFP_{T2}$. If FRET is present, the donor emission

increases when the acceptor is photobleached; we thus expect CFP_{T2} to be bigger than CFP_{T1} (photobleaching interval), and CFP_{T2} to be bigger than CFP_{T3} (no photo-bleaching). In this case, the difference calculated, $(CFP_{T3}/CFP_{T2}) - (CFP_{T2}/CFP_{T1})$ will be negative. Experiments were repeated at least five times per strain with a minimum of 10 cells analyzed per experiment. Analysis was performed in MatLab (code available on request).

Supplementary Material

Refer to Web version on PubMed Central for supplementary material.

Acknowledgments

We thank Dave Popham and members of our laboratory for comments on the manuscript. This work was funded by NIH grant R01GM081368 and by an Irma T. Hirschl Scholar award to J.D. A.J.F. was supported by NIH training grant AI007161-29 and P.M. was supported by a Helen Hay Whitney Fellowship.

REFERENCES

1. van Heijenoort J. Recent advances in the formation of the bacterial peptidoglycan monomer unit. Nat Prod Rep. 2001; 18:503–19. [PubMed: 11699883]
2. Gerard P, Vernet T, Zapun A. Membrane topology of the Streptococcus pneumoniae FtsW division protein. J Bacteriol. 2002; 184:1925–31. [PubMed: 11889099]
3. Lara B, Ayala JA. Topological characterization of the essential Escherichia coli cell division protein FtsW. FEMS Microbiol Lett. 2002; 216:23–32. [PubMed: 12423747]
4. Real G, Fay A, Eldar A, Pinto SM, Henriques AO, Dworkin J. Determinants for the subcellular localization and function of a nonessential SEDS protein. J Bacteriol. 2008; 190:363–76. [PubMed: 17981970]
5. Ikeda M, Sato T, Wachi M, Jung HK, Ishino F, Kobayashi Y, Matsuhashi M. Structural similarity among Escherichia coli FtsW and RodA proteins and Bacillus subtilis SpoVE protein, which function in cell division, cell elongation, and spore formation, respectively. J Bacteriol. 1989; 171:6375–8. [PubMed: 2509435]
6. Henriques AO, Glaser P, Piggot PJ, Moran CP Jr. Control of cell shape and elongation by the rodA gene in Bacillus subtilis. Mol Microbiol. 1998; 28:235–47. [PubMed: 9622350]
7. Ishino F, Park W, Tomioka S, Tamaki S, Takase I, Kunugita K, Matsuzawa H, Asoh S, Ohta T, Spratt BG, et al. Peptidoglycan synthetic activities in membranes of Escherichia coli caused by overproduction of penicillin-binding protein 2 and rodA protein. J Biol Chem. 1986; 261:7024–31. [PubMed: 3009484]
8. Holtje JV. Growth of the stress-bearing and shape-maintaining murein sacculus of Escherichia coli. Microbiol Mol Biol Rev. 1998; 62:181–203. [PubMed: 9529891]
9. Khattar MM, Addinall SG, Stedul KH, Boyle DS, Lutkenhaus J, Donachie WD. Two polypeptide products of the Escherichia coli cell division gene ftsW and a possible role for FtsW in FtsZ function. J Bacteriol. 1997; 179:784–93. [PubMed: 9006034]
10. Khattar MM, Begg KJ, Donachie WD. Identification of FtsW and characterization of a new ftsW division mutant of Escherichia coli. J Bacteriol. 1994; 176:7140–7. [PubMed: 7961485]
11. Boyle DS, Khattar MM, Addinall SG, Lutkenhaus J, Donachie WD. ftsW is an essential cell-division gene in Escherichia coli. Mol Microbiol. 1997; 24:1263–73. [PubMed: 9218774]
12. Vasudevan P, Weaver A, Reichert ED, Linnstaedt SD, Popham DL. Spore cortex formation in Bacillus subtilis is regulated by accumulation of peptidoglycan precursors under the control of sigma K. Mol Microbiol. 2007; 65:1582–94. [PubMed: 17714441]
13. Nakagawa J, Tamaki S, Tomioka S, Matsuhashi M. Functional biosynthesis of cell wall peptidoglycan by polymorphic bifunctional polypeptides. Penicillin-binding protein 1Bs of Escherichia coli with activities of transglycosylase and transpeptidase. J Biol Chem. 1984; 259:13937–46. [PubMed: 6389538]

14. Ishino F, Mitsui K, Tamaki S, Matsuhashi M. Dual enzyme activities of cell wall peptidoglycan synthesis, peptidoglycan transglycosylase and penicillin-sensitive transpeptidase, in purified preparations of Escherichia coli penicillin-binding protein 1A. Biochem Biophys Res Commun. 1980; 97:287–93. [PubMed: 7006606]
15. Suzuki H, van Heijenoort Y, Tamura T, Mizoguchi J, Hirota Y, van Heijenoort J. In vitro peptidoglycan polymerization catalysed by penicillin binding protein 1b of Escherichia coli K-12. FEBS Lett. 1980; 110:245–9. [PubMed: 6989636]
16. Popham DL, Setlow P. Cloning, nucleotide sequence, and regulation of the Bacillus subtilis pbpF gene, which codes for a putative class A high-molecular-weight penicillin-binding protein. J Bacteriol. 1993; 175:4870–6. [PubMed: 8335642]
17. Suzuki H, Nishimura Y, Hirota Y. On the process of cellular division in Escherichia coli: a series of mutants of E. coli altered in the penicillin-binding proteins. Proc Natl Acad Sci U S A. 1978; 75:664–8. [PubMed: 345275]
18. Sauvage E, Kerff F, Terrak M, Ayala JA, Charlier P. The penicillin-binding proteins: structure and role in peptidoglycan biosynthesis. FEMS Microbiol Rev. 2008; 32:234–58. [PubMed: 18266856]
19. Adam M, Fraipont C, Rhazi N, Nguyen-Disteche M, Lakaye B, Frere JM, Devreese B, Van Beeumen J, van Heijenoort Y, van Heijenoort J, Ghuysen JM. The bimodular G57-V577 polypeptide chain of the class B penicillin-binding protein 3 of Escherichia coli catalyzes peptide bond formation from thiolesters and does not catalyze glycan chain polymerization from the lipid II intermediate. J Bacteriol. 1997; 179:6005–9. [PubMed: 9324244]
20. Zhao G, Yeh WK, Carnahan RH, Flokowitsch J, Meier TI, Alborn WE Jr. Becker GW, Jaskunas SR. Biochemical characterization of penicillin-resistant and -sensitive penicillin-binding protein 2x transpeptidase activities of Streptococcus pneumoniae and mechanistic implications in bacterial resistance to beta-lactam antibiotics. J Bacteriol. 1997; 179:4901–8. [PubMed: 9244281]
21. Pisabarro AG, Prats R, Vaquez D, Rodriguez-Tebar A. Activity of penicillin-binding protein 3 from Escherichia coli. J Bacteriol. 1986; 168:199–206. [PubMed: 3531167]
22. Alaedini A, Day RA. Identification of two penicillin-binding multienzyme complexes in Haemophilus influenzae. Biochem Biophys Res Commun. 1999; 264:191–5. [PubMed: 10527863]
23. Begg KJ, Spratt BG, Donachie WD. Interaction between membrane proteins PBP3 and rodA is required for normal cell shape and division in Escherichia coli. J Bacteriol. 1986; 167:1004–8. [PubMed: 3017915]
24. Karimova G, Dautin N, Ladant D. Interaction network among Escherichia coli membrane proteins involved in cell division as revealed by bacterial two-hybrid analysis. J Bacteriol. 2005; 187:2233–43. [PubMed: 15774864]
25. Datta P, Dasgupta A, Singh AK, Mukherjee P, Kundu M, Basu J. Interaction between FtsW and penicillin-binding protein 3 (PBP3) directs PBP3 to mid-cell, controls cell septation and mediates the formation of a trimeric complex involving FtsZ, FtsW and PBP3 in mycobacteria. Mol Microbiol. 2006; 62:1655–73. [PubMed: 17427288]
26. Pastoret S, Fraipont C, den Blaauwen T, Wolf B, Aarsman ME, Piette A, Thomas A, Brasseur R, Nguyen-Disteche M. Functional analysis of the cell division protein FtsW of Escherichia coli. J Bacteriol. 2004; 186:8370–9. [PubMed: 15576787]
27. Henriques AO, de Lencastre H, Piggot PJ. A Bacillus subtilis morphogene cluster that includes spoVE is homologous to the mra region of Escherichia coli. Biochimie. 1992; 74:735–48. [PubMed: 1391053]
28. Daniel RA, Drake S, Buchanan CE, Scholle R, Errington J. The Bacillus subtilis spoVD gene encodes a mother-cell-specific penicillin-binding protein required for spore morphogenesis. J Mol Biol. 1994; 235:209–20. [PubMed: 8289242]
29. Piggot PJ, Coote JG. Genetic aspects of bacterial endospore formation. Bacteriol Rev. 1976; 40:908–62. [PubMed: 12736]
30. Eichenberger P, Jensen ST, Conlon EM, van Ooij C, Silvaggi J, Gonzalez-Pastor JE, Fujita M, Ben-Yehuda S, Stragier P, Liu JS, Losick R. The sigmaE regulon and the identification of additional sporulation genes in Bacillus subtilis. J Mol Biol. 2003; 327:945–72. [PubMed: 12662922]

31. Mercer KL, Weiss DS. The Escherichia coli cell division protein FtsW is required to recruit its cognate transpeptidase, FtsI (PBP3), to the division site. J Bacteriol. 2002; 184:904–12. [PubMed: 11807049]
32. Akiyama Y, Kihara A, Tokuda H, Ito K. FtsH (HflB) is an ATP-dependent protease selectively acting on SecY and some other membrane proteins. J Biol Chem. 1996; 271:31196–201. [PubMed: 8940120]
33. Sloma A, Rufo GA Jr. Theriault KA, Dwyer M, Wilson SW, Pero J. Cloning and characterization of the gene for an additional extracellular serine protease of Bacillus subtilis. J Bacteriol. 1991; 173:6889–95. [PubMed: 1938892]
34. Scheffers DJ, Jones LJ, Errington J. Several distinct localization patterns for penicillin-binding proteins in Bacillus subtilis. Mol Microbiol. 2004; 51:749–64. [PubMed: 14731276]
35. Rubio A, Pogliano K. Septal localization of forespore membrane proteins during engulfment in Bacillus subtilis. Embo J. 2004; 23:1636–46. [PubMed: 15044948]
36. Miyawaki A, Tsien RY. Monitoring protein conformations and interactions by fluorescence resonance energy transfer between mutants of green fluorescent protein. Methods Enzymol. 2000; 327:472–500. [PubMed: 11045004]
37. Bowler LD, Spratt BG. Membrane topology of penicillin-binding protein 3 of Escherichia coli. Mol Microbiol. 1989; 3:1277–86. [PubMed: 2677607]
38. McLeod MP, Warren RL, Hsiao WW, Araki N, Myhre M, Fernandes C, Miyazawa D, Wong W, Lillquist AL, Wang D, Dosanjh M, Hara H, Petrescu A, Morin RD, Yang G, Stott JM, Schein JE, Shin H, Smailus D, Siddiqui AS, Marra MA, Jones SJ, Holt R, Brinkman FS, Miyauchi K, Fukuda M, Davies JE, Mohn WW, Eltis LD. The complete genome of Rhodococcus sp. RHA1 provides insights into a catabolic powerhouse. Proc Natl Acad Sci U S A. 2006; 103:15582–7. [PubMed: 17030794]
39. Marrec-Fairley M, Piette A, Gallet X, Brasseur R, Hara H, Fraipont C, Ghuysen JM, Nguyen-Disteche M. Differential functionalities of amphiphilic peptide segments of the cell-septation penicillin-binding protein 3 of Escherichia coli. Mol Microbiol. 2000; 37:1019–31. [PubMed: 10972821]
40. Piette A, Fraipont C, Den Blaauwen T, Aarsman ME, Pastoret S, Nguyen-Disteche M. Structural determinants required to target penicillin-binding protein 3 to the septum of Escherichia coli. J Bacteriol. 2004; 186:6110–7. [PubMed: 15342580]
41. Yanouri A, Daniel RA, Errington J, Buchanan CE. Cloning and sequencing of the cell division gene pbpB, which encodes penicillin-binding protein 2B in Bacillus subtilis. J Bacteriol. 1993; 175:7604–16. [PubMed: 8244929]
42. Dessen A, Mouz N, Gordon E, Hopkins J, Dideberg O. Crystal structure of PBP2x from a highly penicillin-resistant Streptococcus pneumoniae clinical isolate: a mosaic framework containing 83 mutations. J Biol Chem. 2001; 276:45106–12. [PubMed: 11553637]
43. Noirclerc-Savoye M, Morlot C, Gerard P, Vernet T, Zapun A. Expression and purification of FtsW and RodA from Streptococcus pneumoniae, two membrane proteins involved in cell division and cell growth, respectively. Protein Expr Purif. 2003; 30:18–25. [PubMed: 12821317]
44. Born P, Breukink E, Vollmer W. In vitro synthesis of cross-linked murein and its attachment to sacculi by PBP1A from Escherichia coli. J Biol Chem. 2006; 281:26985–93. [PubMed: 16840781]
45. Bertsche U, Kast T, Wolf B, Fraipont C, Aarsman ME, Kannenberg K, von Rechenberg M, Nguyen-Disteche M, den Blaauwen T, Holtje JV, Vollmer W. Interaction between two murein (peptidoglycan) synthases, PBP3 and PBP1B, in Escherichia coli. Mol Microbiol. 2006; 61:675–690. [PubMed: 16803586]
46. Popham DL. Specialized peptidoglycan of the bacterial endospore: the inner wall of the lockbox. Cell Mol Life Sci. 2002; 59:426–33. [PubMed: 11964121]
47. Daniel RA, Errington J. Control of cell morphogenesis in bacteria: two distinct ways to make a rod-shaped cell. Cell. 2003; 113:767–76. [PubMed: 12809607]
48. Tiyanont K, Doan T, Lazarus MB, Fang X, Rudner DZ, Walker S. Imaging peptidoglycan biosynthesis in Bacillus subtilis with fluorescent antibiotics. Proc Natl Acad Sci U S A. 2006; 103:11033–8. [PubMed: 16832063]

49. Severinov K, Mooney R, Darst SA, Landick R. Tethering of the large subunits of Escherichia coli RNA polymerase. J Biol Chem. 1997; 272:24137–40. [PubMed: 9305860]
50. Zakharova N, Hoffman PS, Berg DE, Severinov K. The largest subunits of RNA polymerase from gastric helicobacters are tethered. J Biol Chem. 1998; 273:19371–4. [PubMed: 9677352]
51. Schwartz B, Markwalder JA, Wang Y. Lipid II: total synthesis of the bacterial cell wall precursor and utilization as a substrate for glycosyltransfer and transpeptidation by penicillin binding protein (PBP) 1b of Escherichia coli. J Am Chem Soc. 2001; 123:11638–43. [PubMed: 11716719]
52. Bertsche U, Breukink E, Kast T, Vollmer W. In vitro murein peptidoglycan synthesis by dimers of the bifunctional transglycosylase-transpeptidase PBP1B from Escherichia coli. J Biol Chem. 2005; 280:38096–101. [PubMed: 16154998]
53. Youngman P, Perkins JB, Losick R. A novel method for the rapid cloning in Escherichia coli of Bacillus subtilis chromosomal DNA adjacent to Tn917 insertions. Mol Gen Genet. 1984; 195:424–33. [PubMed: 6088944]
54. Harwood, CR.; Cutting, SM., editors. Molecular biological methods for Bacillus Modern Microbiological Methods. Wiley; New York: 1990.
55. Sterlini JM, Mandelstam J. Commitment to sporulation in Bacillus subtilis and its relationship to development of actinomycin resistance. Biochem J. 1969; 113:29–37. [PubMed: 4185146]
56. Kodama T, Takamatsu H, Asai K, Kobayashi K, Ogasawara N, Watabe K. The Bacillus subtilis yaaH gene is transcribed by SigE RNA polymerase during sporulation, and its product is involved in germination of spores. J Bacteriol. 1999; 181:4584–91. [PubMed: 10419957]
57. Horton RM, Cai ZL, Ho SN, Pease LR. Gene splicing by overlap extension: tailor-made genes using the polymerase chain reaction. Biotechniques. 1990; 8:528–35. [PubMed: 2357375]

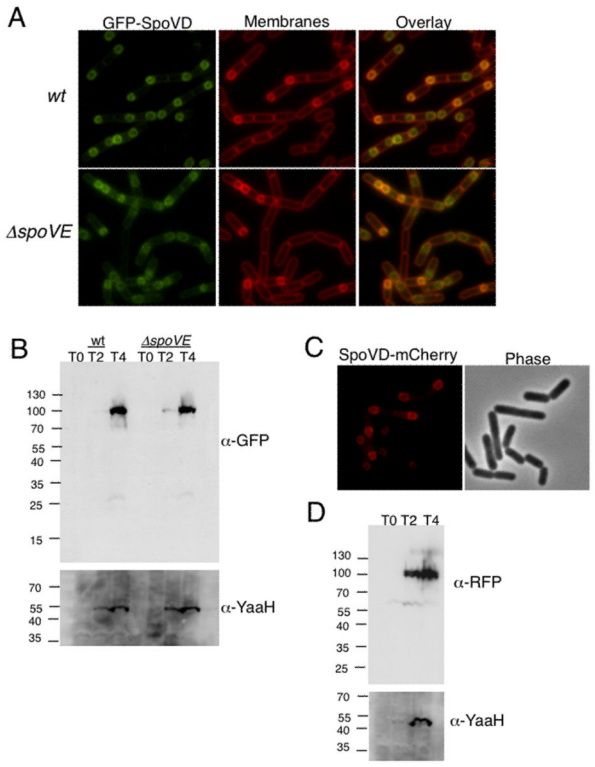

Fig. 1. SpoVD localizes to the outer forespore membrane

A. GFP-SpoVD requires SpoVE for recruitment to outer forespore membrane. Samples of JDB1327 (wt) and JDB2026 (Δ*spoVE)* were obtained at T3 of sporulation by resuspension and prepared for fluorescence microscopy. Bacterial membranes were visualized with FM4-64 (1μg/ml). *B.* GFP-SpoVD accumulates at full length in a *spoVE* mutant. Strains were sporulated by resuspension and samples taken at T0, T2, and T4 were normalized to efficiency, anti-YaaH was used. *C*. SpoVD-mCherry localizes to the outer forespore membrane. Samples of JDB2363 (*spoVD-mCherry*) were obtained at T3 of sporulation by resuspension and prepared for fluorescence microscopy. *D*. SpoVD-mCherry accumulates at the predicted size. JDB2363 was sporulated by resuspension and samples taken at T0, T2, and T4 were normalized to OD600 and subjected to 12% SDS-PAGE and probed with anti-RFP. As a control for sporulation efficiency, anti-YaaH was used.

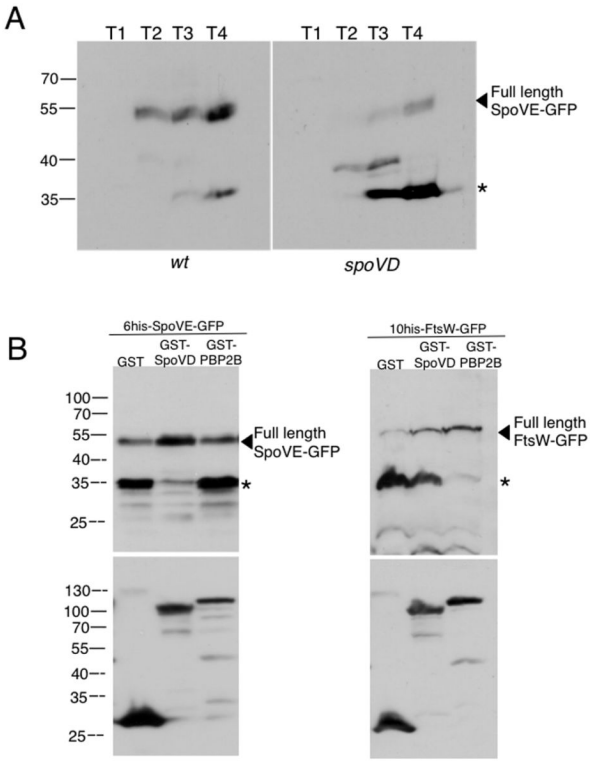

Fig. 2. Stability of SpoVE is dependent on SpoVD

A. SpoVE-GFP is unstable in a *spoVD* mutant. Strains JDB1933 (wt) and JDB2148 (*spoVD*) were sporulated by resuspension. Samples taken at each time point were normalized to an OD_{600} and lysates were subjected to 13.5% SDS-PAGE and probed with anti-GFP followed by anti-rabbit-HRP and detected by ECL. The arrowhead indicates full-length product, while the asterisk indicates the main cleavage product. *B.* SEDS proteins require their specific PBP for stability when expressed in a heterologous system. *E. coli* BL21 strains were induced for 2h with 0.1% arabinose at 25°C. Pellets containing equivalent amounts of cells (as by determined OD_{600}) were solubilized in 1x sample buffer at RT and subjected to 13.5% SDS-PAGE. After transfer to nitrocellulose, the blot was probed with anti-GFP, anti-rabbit-HRP, ECL plus, then stripped and probed with anti-GST, anti-rabbit-HRP to verify GST fusion expression. Full-length product is indicated by an arrowhead and the main cleavage product is indicated by an asterisk. SpoVE-GFP is stabilized by GST-SpoVD expression, but not by GST-PBP2B. FtsW-GFP is stabilized by GST-PBP2B, but not by GST-SpoVD.

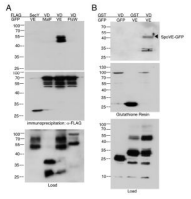

Fig. 3. Interaction between SpoVE and SpoVD

A. SpoVE-GFP co-immunoprecipitates with SpoVD-FLAG in *B. subtilis*. Strains expressing combinations of GFP and FLAG fusion proteins were sporulated by resuspension and lysates from samples taken at T2.5 were solubilized in 1% NP-40 and immunoprecipitated with M2 Affinity resin (Sigma). Lysates and eluates were subjected to 13.5% SDS-PAGE, and blots were probed with anti-GFP (top and bottom) or anti-FLAG (middle), anti-rabbit-HRP (Pierce), and detected with ECL. SpoVD-FLAG co-immunoprecipitated SpoVEGFP (lane 3; JDB1676) but not MalF-GFP (lane 2; JDB1665) or FtsW-GFP (lane 4; JDB1885). SecY-FLAG did not co-immunoprecipitate SpoVE-GFP (lane 1; JDB2155). *B.* SpoVE-GFP co-affinity purifies with GST-SpoVD. *E. coli* BL21 strains expressing GFP and GST tagged proteins were grown in LB at 37°C and induced for 120 min with 0.1% arabinose at OD_{600}=0.8. Samples were collected and lysates containing equivalent amounts of cells (as by determined OD_{600}) were solubilized with 1% NP-40 before affinity purification using immobilized glutathione. Lysates and eluates were subjected to 13.5% SDS-PAGE. After transfer to nitrocellulose, the blots were probed with anti-GFP and anti-rabbit-HRP (top and bottom), then stripped and probed with anti-GST and anti-rabbit-HRP (middle). GST-SpoVD co-affinity purified with SpoVE-GFP (lane 3; JDE1043) but not GFP alone (lane 1; JDE1045). In addition, GST alone did not co-affinity purify SpoVE-GFP (lane 2; JDE1044).

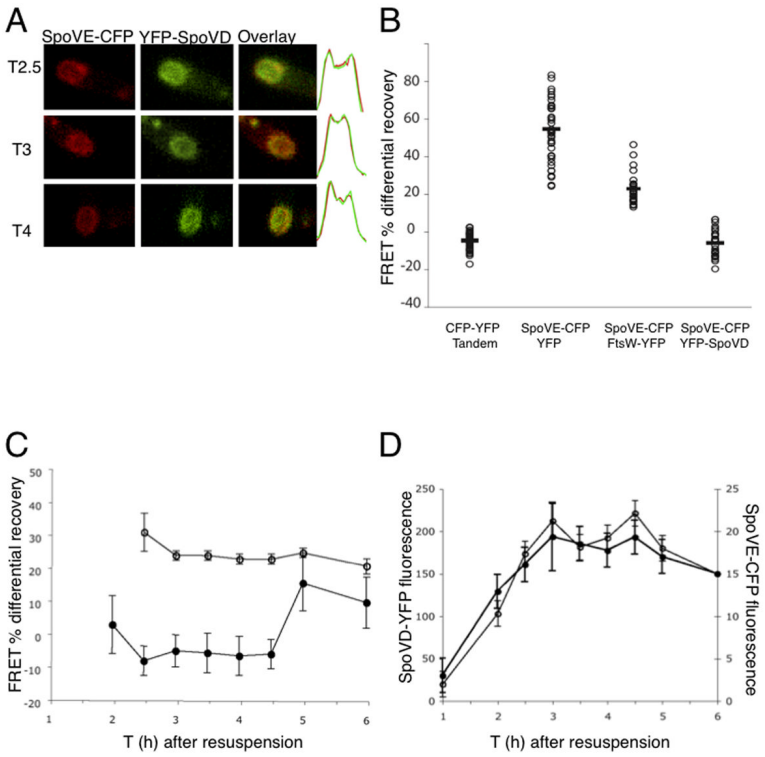

Fig. 4. FRET assay of SpoVE and SpoVD interaction *in vivo*

A. Strain JDB1467 expressing SpoVE-CFP and YFP-SpoVD was sporulated by resuspension at 37°C and samples taken at T2.5, T3 and T4 of sporulation were prepared for fluorescence microscopy. Left panel (red) show SpoVE-CFP images, middle panel (green) YFP-SpoVD and right panel is the overlay. Far right, green and red graphs represent the overlay of the fluorescence distributions of SpoVE-CFP and YFP-SpoVD, y-axis shows fluorescence intensity in arbitrary units and the x-axis is the spore length. *B.* FRET was measured for single cells (~40) of strains expressing CFP and YFP CFP); JDB2158 (SpoVE-CFP, FtsW-YFP); and JDB1467 (SpoVE-CFP, YFP-SpoVD). *C.* FRET was measured for single cells of strains JDB1467 (filled circles; SpoVE-CFP, YFP-SpoVD) and JDB1988 (open circles; free CFP, YFP) at specified times during sporulation by resuspension at 37°C. FRET measurements were significantly different between the two strains ($p<.001$) for all times between T2 and T4.5. *D.* Strain JDB1467 (SpoVE-CFP, YFP-SpoVD) was sporulated by resuspension and fluorescence levels of SpoVE-CFP (closed circles) and YFP-SpoVD (open circles) was measured in ~50 single cells.

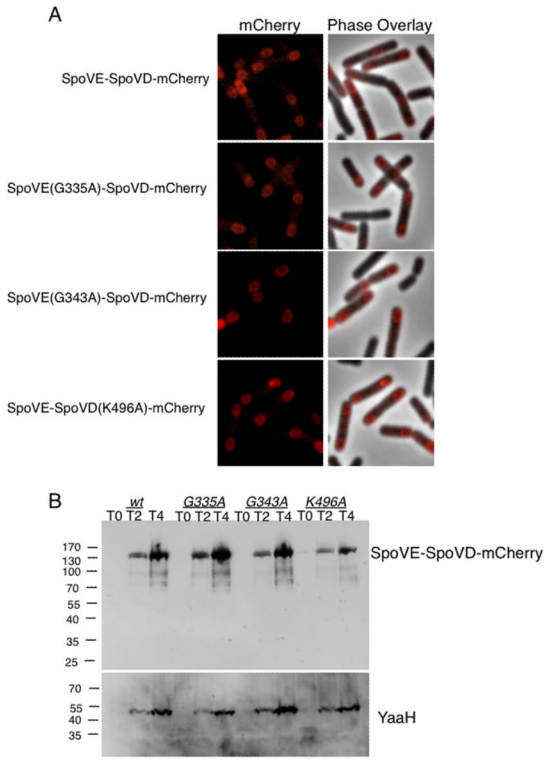

Fig. 5. Localization of wild type and mutant SpoVE-SpoVD fusion proteins

A. SpoVE-SpoVD-mCherry wild type and mutant fusion proteins are recruited to the outer forespore membrane. Cells of JDB2647 (wt), JDB2661 (*spoVE(G335A)-spoVD-mCherry*) JDB2662 (*spoVE(G343A)-spoVD-mCherry*) JDB2665 (*spoVE-spoVD(K496A)-mCherry*) at T3 of sporulation by resuspension were prepared for fluorescence microscopy. *B.* SpoVE-SpoVD-mCherry point mutants accumulate to the predicted size. Strains sporulated by resuspension and samples taken at T0, T2, and T4 were normalized to OD_{600} and subjected to 12% SDS-PAGE and probed with anti-RFP. As a control for sporulation efficiency, anti-YaaH was used.

Table 1

Bacterial strains.

Strain	*Genotype*	Source
B. subtilis		
PY79	*wt*	Lab stock
JDB223	*ftsW-gfp spc*	4
JDB361	*amyE::P_{ftsW}-ftsW-gfp cm*	this work
JDB389	*ftsW::tet amyE::P_{ftsW}-ftsW-gfp cm*	this work
JDB646	*spoVE::neo*	4
JDB1134	*spoVE::neo amyE::P_{spoVE}-spoVE-gfp spc cm*	4
JDB1213	*spoVD::kan*	28
JDB1240	*spoVE::neo::spc*	this work
JDB1327	*spoVD::kan amyE::P_{spoVE}-gfp-spoVD cm*	this work
JDB1376	*spoVE::neo amyE::P_{spoVE}-spoVE-cfp spc cm*	4
JDB1396	*pyrD::P_{spoIID}-yfp cm*	this work
JDB1440	*spoVE::neo amyE::P_{spoVE}-spoVE-cfp spc*	this work
JDB1448	*gltA::P_{spoVE}-yfp-spoVD cm*	this work
JDB1451	*gltA::P_{spoVE}-yfp-spoVD mls*	this work
JDB1457	*gltA::P_{spoVE}-yfp-spoVD mls spoVE::neo amyE::P_{spoVE}-spoVE-cfp spc*	this work
JDB1467	*spoVD::kan gltA::P_{spoVE}-yfp-spoVD mls spoVE::neo amyE::P_{spoVE}-spoVE-cfp spc*	this work
JDB1495	*spoVE::neo::spc amyE:P_{spoVE}-spoVE-cfp spc cm, sacA::P_{spoIIQ}-yfp kan*	this work
JDB1559	*ftsW-yfp spc*	this work
JDB1636	*spoVD-flag tet*	this work
JDB1637	*amyE::P_{spoIIQ}-malF(1,2)-gfp cm*	35
JDB1665	*spoVD-flag tet amyE::P_{spoIIQ}-malF(1,2)-gfp cm*	this work
JDB1676	*spoVE::neo spoVD-flag tet amyE::P_{spoVE}-spoVE-gfp spc cm*	this work
JDB1686	*sacA::P_{spoIID}-cfp tet*	this work
JDB1725	*Sac:A:P_{spoVE}-spoVE-cfp tet*	this work
JDB1752	*ΔspoVE::tet*	4
JDB1885	*ftsW-gfp spc spoVD-flag tet*	this work
JDB1904	*amyE::P_{spoVE}-yfp-cfp cm*	this work
JDB1918	*ΔspoVE::tet spoVD::kan*	this work
JDB1933	*ΔspoVE::tet amyE::P_{spoVE}-spoVE-gfp cm*	4
JDB1988	*pyrD::P_{spoIID}-yfp cm sacA::P_{spoIID}-cfp tet*	this work
JDB2026	*ΔspoVE::tet spoVD::kan amyE::P_{spoVE}-gfp-spoVD cm*	this work
JDB2059	*ΔspoVE:: tet spoVD::kan amyE::P_{spoVE}-gfp-spoVD cm sacA::P_{spoVE}-spoVE(G334A) mls*	this work
JDB2061	*ΔspoVE:: tet spoVD::kan amyE::P_{spoVE}-gfp-spoVD cm sacA::P_{spoVE}-spoVE(G343A) mls*	this work
JDB2063	*ΔspoVE:: tet spoVD::kan amyE::P_{spoVE}-gfp-spoVD cm sacA::P_{spoVE}-spoVE(E271A) mls*	this work

Strain	*Genotype*	Source
JDB2064	*ΔspoVE:: tet spoVD::kan amyE::P_{spoVE}-gfp-spoVD cm sacA::P_{spoVE}-spoVE(W69A) mls*	this work
JDB2148	*ΔspoVE::tet spoVD::kan amyE::P_{spoVE}-spoVE-gfp cm*	this work
JDB2155	*ΔspoVE::tet amyE::P_{spoVE}-spoVE-gfp cm sacA::P_{spoVE}-secY(1,6)-flag mls*	this work
JDB2158	*amyE::P_{spoVE}-ftsW-yfp cm sacA::P_{spoVE}-spoVE-cfp tet*	this work
JDB2171	*amyE::P_{spoVE}-ftsW-yfp cm*	this work
JDB2200	*amyE::P_{spoVE}-spoVE-GSGSGS-spoVD-flag cm*	this work
JDB2201	*ΔspoVE::tet spoVD::kan amyE::P_{spoVE}-spoVE-GSGSGS-spoVD-flag cm*	this work
JDB2203	*ΔspoVE::tet spoVD::kan amyE::P_{spoVE}-spoVE(G343A)-GSGSGS-spoVD-flag cm*	this work
JDB2255	*ΔspoVE::tet spoVD::kan amyE::P_{spoVE}-spoVE-GSGSGS-pbpB-flag cm*	this work
JDB2256	*amyE::P_{ftsW}-ftsW-GSGSGS-pbpB-flag cm*	this work
JDB2267	*ΔspoVE::tet spoVD::kan amyE::P_{spoVE}-spoVE-GSGSGS-spoVD(K496A)-flag cm*	this work
JDB2269	*ΔspoVE::tet amyE::P_{spoVE}-spoVE-GSGSGS-spoVD(K496A)-flag cm*	this work
JDB2269	*ΔspoVE::tet amyE::P_{spoVE}-spoVE-GSGSGS-spoVD(K496A)-flag cm*	this work
JDB2272	*spoVD::kan amyE::P_{spoVE}-spoVE(G343A)-GSGSGS-spoVD-flag cm*	this work
JDB2279	*spoVD::kan amyE::P_{spoVE}-spoVE(G334A)-GSGSGS-spoVD-flag cm*	this work
JDB2280	*spoVD::kan amyE::P_{spoVE}-spoVE(E271A)-GSGSGS-spoVD-flag cm*	this work
JDB2322	*ΔspoVE::tet spoVD::kan amyE::P_{spoVE}-spoVE-spoVD(Q227E)-flag cm*	this work
JDB2363	*spoVD-mCherry spc*	this work
JDB2367	*ΔspoVE::tet amyE::Ps_{spoVE}-spoVE-GSGSGS-pbpB-flag cm*	this work
JDB2440	*ftsW::tet ΔpbpB::mls amyE::P_{ftsW}-ftsW-GSGSGS-pbpB-flag cm*	this work
JDB2647	*ΔspoVE::tet spoVD::kan amyE::P_{spoVE}-spoVE-GSGSGS-spoVD-mCherry spc cm*	this work
JDB2661	*ΔspoVE::tet spoVD::kan amyE::P_{spoVE}-spoVE(G335A)-GSGSGS-spoVD-mCherry spc cm*	this work
JDB2662	*ΔspoVE::tet spoVD::kan amyE::P_{spoVE}-spoVE(G343A)-GSGSGS-spoVD-mCherry spc cm*	this work
JDB2665	*ΔspoVE::tet amyE::P_{spoVE}-spoVE-GSGSGS-spoVD(K496A)-mCherry spc cm*	this work
E. coli		
BL21(DE3)		Lab stock
JDE1038	*pAF188(P_{ara}-6his-spoVE-gfp araC cm), pAF172 (P_{ara}-gst araC bla)*	this work
JDE1039	*pAF188(P_{ara}-6his-spoVE-gfp araC cm), pAF175(P_{ara}-gst-spoVD araC bla)*	this work
JDE1040	*pAF188(P_{ara}-6his-spoVE-gfp araC cm), pAF267(P_{ara}-gst-pbpB araC bla)*	this work
JDE1041	*pAF256(P_{ara}-10his-ftsW-gfp araC cm), pAF175 pAF175(P_{ara}-gst-spoVD araC bla)*	this work
JDE1042	*pAF256(P_{ara}-10his-ftsW-gfp araC cm), pAF267(P_{ara}-gst-pbpB araC bla)*	this work
JDE1043	*pAF191(P_{ara}-10his-spoVE-gfp araC bla), pAF231(P_{ara}-gst-spoVD araC cm)*	this work
JDE1044	*pAF191(P_{ara}-10his-spoVE-gfp araC bla), pAF232 (P_{ara}-gst araC cm)*	this work
JDE1045	*pAF233(P_{ara}-10his-gfp araC bla), pAF231(P_{ara}-gst-spoVD araC cm)*	this work
JDE1307	*pAF256(P_{ara}-10his-ftsW-gfp araC cm), pAF175 pAF172(P_{ara}-gst araC bla)*	this work

Table 2

GFP-SpoVD recruitment to the forespore at T3 of sporulation.

***spoVE* allele**	**GFP-SpoVD signal (forespore:mothercell)**
wt	3.27 +/− .76
ΔspoVE::tet	1.99 +/− .26
spoVE(G334A)	3.21 +/− .53
spoVE(G343A)	3.23 +/− .46
spoVE(E271A)	3.25 +/− .63
spoVE(W69A)	2.10 +/− .24

Table 3

Sporulation of *B. subtilis* strains expressing SpoVD-SpoVE fusions.

Genotype	CFU/ml pre-heat	CFU/ml post-heat	% Sporulation
Wild type	2.9×10^{8}	2.7×10^{8}	90 ± 4.7
ΔspoVE::tet spoVD::kan	5.0×10^{7}	0	0
ΔspoVE::tet spoVD::kan amyE::P_{spoVE}-spoVE-spoVD-flag	2.8×10^{8}	2.5×10^{8}	89 ± 5.4
ΔspoVE::tet spoVD::kan amyE::P_{spoVE}-spoVE(G343A)-spoVD-flag	4.7×10^{7}	321	6.5×10^{-4} ± 0.7 $\times10^{-4}$
spoVD::kan amyE::P_{spoVE}-spoVE(G343A)-spoVD-flag	3.4×10^{7}	455	1.4×10^{-3} ± 0.9 $\times10^{-3}$
spoVD::kan amyE::P_{spoVE}-spoVE(G335A)-spoVD-flag cm	8.3×10^{7}	690	8.6×10^{-4} ± 1.3×10^{-4}
spoVD::kan amyE::P_{spoVE}-spoVE(E271A)-spoVD-flag	7.1×10^{7}	600	8.2×10^{-4} ± 0.9 $\times10^{-4}$
ΔspoVE::tet spoVD::kan amyE::P_{spoVE}-spoVE-spoVD(K496A)-flag	5.4×10^{7}	750	1.3×10^{-3} ± 2.1 $\times10^{-3}$
ΔspoVE::tet amyE::P_{spoVE}-spoVE-spoVD(K496A)-flag	5.8×10^{7}	890	1.2×10^{-3} ± 0.7 $\times10^{-3}$
ΔspoVE::tet spoVD::kan amyE::P_{spoVE}-spoVE-pbpB-flag	6.1×10^{7}	0	0
ΔspoVE::tet amyE::P_{spoVE}-spoVE-pbpB-flag	2.6×10^{8}	5.0×10^{5}	0.19 ± 0.05
ΔspoVE::tet spoVD::kan amyE::P_{spoVE}-spoVE-spoVD(Q227E)-flag	3.5×10^{8}	3.3×10^{8}	88 ± 6.5

[1] CFU data represents one typical heat kill experiment and percent sporulation represents an average from three experiments. Each strain was grown in DSM for 24h at 37°C, then exposed to 80°C for 20 min.